12-2012

PDMS$_{star}$-PEG Hydrogels Prepared Via Solvent-Induced Phase Separation (SIPS) and Their Potential Utility as Tissue Engineering Scaffolds

B. M. Bailey

R. Fei

Dany J. Munoz Pinto
Trinity University, dmunozpi@trinity.edu

M. S. Hahn

M. A. Grunlan

Repository Citation

Bailey, B. M., Fei, R., Munoz-Pinto, D., Hahn, M. S., & Grunlan, M. A. (2012). PDMSstar-PEG hydrogels prepared via solvent-induced phase separation (SIPS) and their potential utility as tissue engineering scaffolds. *Acta Biomaterialia, 8*(12), 4324-4333. doi:10.1016/j.actbio.2012.07.034

HHS Public Access

Author manuscript

Acta Biomater. Author manuscript; available in PMC 2019 March 16.

Published in final edited form as:

Acta Biomater. 2012 December ; 8(12): 4324–4333. doi:10.1016/j.actbio.2012.07.034.

$PDMS_{star}$-PEG Hydrogels Prepared via Solvent-Induced Phase Separation (SIPS) and Their Potential Utility as Tissue Engineering Scaffolds

Brennan M. Bailey[a,b], **Ruochong Fei**[a], **Dany Munoz-Pinto**[c], **Mariah S. Hahn**[b,c], and **Melissa A. Grunlan**[a,b]

[a]Department of Biomedical Engineering, Texas A&M University, College Station, TX, 77843-3120, USA

[b]Materials Science and Engineering Program, Texas A&M University, College Station, TX, 77843-3120, USA

[c]Department of Chemical Engineering, Texas A&M University, College Station, TX, 77843-3120, USA

Abstract

Inorganic-organic hydrogels based on methacrylated star polydimethylsiloxane ($PDMS_{star}$-MA) and diacrylated poly(ethylene glycol) (PEG-DA) macromers were prepared via solvent-induced phase separation (SIPS). The macromers were combined in a dichloromethane (DCM) precursor solution and sequentially photopolymerized, dried and hydrated. The chemical and physical properties of the hydrogels were further tailored by varying the number average molecular weight (M_n) of PEG-DA (M_n = 3.4k and 6k g/mol) as well as the weight % (wt%) ratio of $PDMS_{star}$-MA (M_n = 7k g/mol) to PEG-DA from 0:100 to 20:80. Compared to analogous hydrogels fabricated from aqueous precursor solutions, SIPS produced hydrogels with a macroporous morphology, a more even distribution of $PDMS_{star}$-MA, increased modulus and enhanced degradation rates. The morphology, swelling ratio, mechanical properties, bioactivity, non-specific protein adhesion, controlled introduction of cell-adhesion, and cytocompatibility of the hydrogels were characterized. As a result of their tunable properties, this library of hydrogels is useful to study material-guided cell behavior and ultimate tissue regeneration.

Keywords

poly(ethylene glycol); polydimethylsiloxane; hydrogel; scaffold; tissue engineering

Corresponding Author - Melissa Grunlan, mgrunlan@tamu.edu, Phone: (979) 845-2406, Fax: (979) 845-4450, Address: Texas A&M University, Biomedical Engineering Department, 5030 Emerging Technologies Building, MS 3120, College Station, TX, 77843-3120.

Appendix A. Supporting Information Available.

Sol content values of hydrogels (Table S1), SEM images of $PDMS_{star}$-PEG hydrogels (Fig. S1) and degradation of "water fabricated" hydrogels (Fig. S2). This material is available free of charge via the Internet at http://www.sciencedirect.com

1. Introduction

In tissue engineering, the properties of the three dimensional scaffold guide cell behavior and ultimate tissue regeneration.[1-5] Physical properties of scaffolds known to impact cell behavior include modulus [6-9] and morphology (e.g. porosity).[10-19] In addition, scaffold chemical properties influence cell behavior including bioactivity,[20-22] chemical functionality,[23] hydrophobicity,[24-26] and related hydration (i.e. swelling).[6, 27] Therefore, a library of scaffolds having precisely tunable physical and chemical properties over a broad range would be a valuable tool to probe material-guided cell behavior and enable the regeneration of functional tissues.

Poly(ethylene glycol) diacrylate (PEG-DA) hydrogels are extensively utilized as scaffolds for the regeneration of numerous types of tissues.[28-34] Their resistance to protein and cell adhesion in the absence of cell adhesive ligands makes them particularly useful to study cell-material interactions.[28-29, 35-37] Thus, changes in cell behavior may be related to an associated material property change. However, PEG-DA hydrogels display a limited range of physical as well as chemical properties restricting their utility for such studies. For instance, the modulus of PEG-DA hydrogels may be tuned over a somewhat narrow range by altering the crosslink density (i.e. PEG-DA number average molecular weight, M_n) or the weight percent (wt%) concentration of PEG-DA in the aqueous precursor solution.[31, 38] However, these alterations simultaneously produce changes in swelling thereby restricting the ability to uncouple the effect of modulus and swelling on cellular response.[39] While morphological changes in general alter cell behavior,[40-42] a macroporous hydrogel morphology has shown particular utility in tissue regeneration.[18, 43-44] PEG-DA (M_n = 3.4k and 6k g/mol) hydrogels fabricated by the photopolymerization of aqueous precursor solutions exhibit pores smaller than ~5-10 μm.[45] Several strategies have been explored to produce macroporous PEG-DA hydrogels, including: salt leaching,[46-47] gas foaming [48] and cryogelation.[49-50] However, difficulty leaching porogens (salt leaching), high temperatures or low pressures (gas foaming), and extremely low temperatures (cryogelation) [51] limits these techniques.

In general, the chemical nature of hydrogel scaffolds has been shown to have a significant impact on cell behavior.[52-56] Alterations to the chemical nature of PEG-DA hydrogels have been largely limited to those that increase the rate of degradation. For instance, polyester segments [57-58] and enzymatically unstable peptides [37, 59] have been introduced to enhance the otherwise limited degradation rate of PEG-DA hydrogels. The impact of chemical functionality incorporated into PEG-DA hydrogels on cell behavior has been explored only to a limited extent.[23] Previous studies have demonstrated that the incorporation of inorganic silicon-containing materials into organic scaffolds enhances their bioactivity.[20-21, 60] In addition, scaffold hydrophobicity has also been shown to influence osteogenic differentiation.[25-26, 61] In our prior report, hydrogels were formed by introduction of an inorganic, hydrophobic methacrylated star polydimethylsiloxane ($PDMS_{star}$-MA) into PEG-DA hydrogels.[62] The insolubility of the $PDMS_{star}$-MA in the aqueous precursor solutions produced hydrogels comprised of discrete $PDMS_{star}$-enriched microparticles distributed throughout the PEG-DA hydrogel matrix. $PDMS_{star}$-MA content altered mechanical behavior without significant changes to hydration. Furthermore, our

previous study showed that these PDMS-PEG hydrogel scaffolds demonstrated the ability to guide mesenchymal stem cells (MSCs) towards osteogenic differentiation with increased levels of $PDMS_{star}$-MA.[63]

Recently, we prepared PEG-DA hydrogels via solvent induced phase separation (SIPS) which involved photopolymerization of a dichloromethane (DCM) precursor solution followed by sequentially drying and hydration.[64] During SIPS, a solvent system is utilized which promotes phase separation of the growing polymer chain and network during cure.[65-66] Compared to PEG-DA hydrogels fabricated from an aqueous precursor solution, hydrogels were macroporous and exhibited increased modulus values and enhanced degradation rates. Herein, we report the introduction of variable levels $PDMS_{star}$-MA into PEG-DA hydrogels fabricated via SIPS to produce bioactive, macroporous $PDMS_{star}$-PEG hydrogel scaffolds with enhanced modulus values and degradation rates. In contrast to $PDMS_{star}$-PEG hydrogels fabricated from an aqueous solvent, the improved solubility of $PDMS_{star}$-MA in the DCM fabrication solvent enables its more homogeneous distribution throughout the hydrogel. A series of $PDMS_{star}$-PEG hydrogels were prepared via SIPS (i.e. from DCM precursor solutions) at 10 wt% total macromer concentration but with variable wt% ratios of $PDMS_{star}$-MA (7k g/mol) to PEG-DA (3.4k and 6k g/mol) [0:100, 1:99, 10:90 and 20:80]. The effect of hydrogel composition on physical and chemical properties, including equilibrium swelling (i.e. hydration), morphology, compressive modulus, degradation, bioactivity, protein resistance, controlled introduction of cell adhesion and cytocompatibility were assessed. Properties of $PDMS_{star}$-PEG hydrogels fabricated via SIPS were compared to analogous hydrogels fabricated from an aqueous precursor solution.

2. Materials and Methods

2.1. Materials

Pt-divinyltetramethyldisiloxane complex (Karstedt's catalyst, 2 wt% in xylene), tetrakis(dimethylsiloxy)silane (tetra-SiH), and octamethylcyclotetrasiloxane (D_4) were obtained from Gelest. Allyl methacrylate, acryloyl chloride, triflic acid, 2,2-dimethyl-2-phenyl-acetophenone (DMAP), 1-vinyl-2-pyrrolidinone (NVP), triethylamine (Et_3N), $MgSO_4$, K_2CO_3, hexamethyldisilazane (HMDS), N3013 Nile Red (Nile Blue A Oxazone), NaOH, and solvents were obtained from Sigma Aldrich. HPLC grade toluene, CH_2Cl_2, and NMR grade $CDCl_3$ were dried over 4Å molecular sieves. Poly(ethylene glycol) (PEG) [PEG-6000; MW = 5000-7000 g/mol and PEG-3400; MW = 3000-3700 g/mol per manufacturer's specifications] were obtained from BioChemika. The M_n of PEG-3400 (3371 g/mol) and PEG-6000 (6072 g/mol) were back-calculated from ^1H NMR end-group analysis of the corresponding diacrylated products. Phosphate buffered solution (PBS, pH = 7.4, without calcium and magnesium), HEPES, Dulbecco's Modified Eagle Medium (DMEM), fetal bovine serum (FBS), PSG solution (10,000 U/mL penicillin, 10000 mg/L streptomycin, and 29.2 mg/mL L-glutamine), and PSA solution (10,000 U/mL penicillin, 10,000 mg/L streptomycin, and 25 mg/L amphotericin) were obtained from Mediatech. Peptide RGDS was obtained from American Peptide. Acryloyl PEG-succinimidyl valerate (acryloyl-PEG-SVA, 3.4 kDa) was obtained from Laysan Bio Inc. Mouse smooth muscle precursor cells (10T1/2) were obtained from American Type Culture Collection (ATCC).

2.2. $PDMS_{star}$-MA Synthesis

$PDMS_{star}$-MA was prepared as previously reported.[67] First, D_4 (29.9 g, 100.8 mmol), tetra-SiH (1.1 g, 3.3 mmol), triflic acid (60 μL), and HMDS (0.15 g, 0.93 mmol) were reacted. In this way, $PDMS_{star}$-SiH (24.9 g, 80% yield) was obtained as a colorless liquid, M_n/M_w = 7600/18,800 g/mol, PDI = 2.5. ^{1}H NMR (δ, ppm): 0.064-0.113 (bm, 1174H, SiCH_3), 4.7 (m, 4H, SiH). IR (ν): 2125 cm-1 (Si-H). Next, $PDMS_{star}$-SiH (7.0 g, 0.92 mmol), allyl methacrylate (0.26 g, 2.1 mmol), toluene (30 mL), and Karstedt's catalyst (100 μL) were reacted to obtain $PDMS_{star}$-MA (6.37 g, 88% yield) as a colorless liquid, M_n/M_w = 8300/22,000 g/mol, PDI = 2.6. ^{1}H NMR (δ, ppm): 0.045-0.127 (bm, 1673H, SiCH_3), 0.559 (m, 8H, -SiCH_2CH$_2$CH$_2$), 1.67 (m, 8H, -SiCH$_2$$CH_2CH_2$), 1.92 (m, 12H, -C(CH$_2$)$CH_3$), 4.10 (m, 8H, -SiCH$_2CH_2$$CH_2$), 5.57 (m, 4H, -C($CH_2$)CH$_3$), 6.11 (m, 4H, -C($CH_2$)CH$_3$). IR (*v*): no Si-H peak.

2.3. PEG-DA Synthesis

PEG-DA (3.4k and 6k g/mol) were prepared as previously reported.[62] PEG-3400 (23.5 g, 7.0 mmol), Et_3N (1.95 mL, 14.0 mmol) and acryloyl chloride (2.27 mL, 28.0 mmol) were reacted to obtain PEG-DA (15.2 g, 63% yield). ^{1}H NMR (δ, ppm): 3.62 (s, 297H, -OCH_2CH_2), 5.81 (dd, 2H, J = 10.5 and 1.2 Hz, -CH=CH_2), 6.13 (dd, 2H, J = 17.4 and 10.5 Hz, -CH=CH_2), 6.40 (dd, 2H, J = 17.3 and 1.5 Hz, -CH=CH_2). By ^{1}H NMR end-group analysis, M_n of PEG-DA (3.4k g/mol) was determined to be 3393 g/mol (~3400 g/mol). PEG-6000 (24 g, 4.0 mmol), Et_3N (1.12 mL, 8.0 mmol) and acryloyl chloride (1.30 mL, 16.0 mmol) were reacted to obtain PEG-DA (31 g, 63% yield). ^{1}H NMR (δ, ppm): 3.61 (s, 547H, -OCH_2CH_2), 5.81 (dd, 2H, J = 10.4 and 1.5 Hz, -CH=CH_2), 6.13 (dd, 2H, J = 16.8 and 10.5 Hz, -CH=CH_2), 6.40 (dd, 2H, J = 17.3 and 1.5 Hz, -CH=CH_2). By ^{1}H NMR end-group analysis, M_n of PEG-DA (6k g/mol) was determined to be 6143 g/mol (~6000 g/mol).

2.4. NMR

^{1}H NMR spectra were obtained on a Mercury 300 300 MHz spectrometer operating in the Fourier transform mode. Five percent (w/v) $CDCl_3$ solutions were used to obtain spectra. Residual $CHCl_3$ served as an internal standard.

2.5. Hydrogel Preparation

$PDMS_{star}$-PEG hydrogels formed via SIPS were prepared from DCM-based precursor solutions and analogous hydrogels were prepared from aqueous precursor solutions at the same concentrations for comparison. First, PEG-DA (3.4k or 6k g/mol) was added to either DCM or DI-H_2O at 10 wt% total concentration in solvent. $PDMS_{star}$-MA (7k g/mol) was then added at the following wt% ratios of $PDMS_{star}$-MA to PEG-DA: 0:100, 1:99, 10:90 and 20:80. 10 μL of photoinitiator solution (30 wt% solution of DMAP in NVP) was subsequently added per one mL of the precursor solution. Solutions were vortexed for one minute following each addition. Planar hydrogel sheets (1.5 mm thick) were prepared by pipetting the precursor solution between two clamped microscope slides (75 × 50 mm) separated by Teflon spacers and exposing the mold to longwave UV light (UV-Transilluminator, 6 mW/cm^2, 365 nm) for a total of 6 min with rotation to the alternate side after 3 min. After removal from the mold, the water-based hydrogel sheets were rinsed with

DI water and soaked in a Petri dish containing DI water (60 mL) for 2 days with daily water changes to remove impurities. The DCM-based sheets were rinsed with DCM then air dried for 30 min to permit evaporation of DCM and subsequently placed in a Petri dish containing DI water (60 mL) to remove impurities and any remaining DCM. During the first hour of soaking, the water was changed every 15 min and thereafter daily for 2 days. All hydrogels were permitted to soak in DI water for 72 hr prior to testing.

2.6. Sol Content

Three discs (13 mm diameter) were punched from a single hydrogel sheet with a die. After air-drying (30 min), each disc was placed in an open scintillation vial and dried at room temperature (RT) in a vacuum oven (14.7 psi, 24 hr). Dried discs were then weighed (W_{d1}), placed in a new vial and 10 mL DCM was added to each. The vials were capped and placed on a rocker table (250 rpm) for 48 hr to remove sol (i.e. uncrosslinked material). The discs were subsequently removed, air dried for 30 min, placed in an open vial, dried again at RT in a vacuum oven (30 in. Hg, 24 hr) and finally weighed (W_{d2}). Sol Content is defined as: sol content = $[(W_{d1} - W_{d2})/W_{d1}] \times 100$.

2.7. Morphology

2.7.1. Scanning Electron Microscopy—

Water-swollen hydrogels discs (13 mm diameter) were flash frozen in liquid nitrogen for 1 min and immediately lyophilized for 24 hr (Labconco Centri Vap Gel Dryer System). Specimen cross-sections were subjected to Pt-sputter coating and viewed with a field emission scanning electron microscope (FEI Quanta 600 FE-SEM) at an accelerated electron energy of 10 keV.

2.7.2. Confocal Laser Scanning Microscopy (CLSM)—

For a given hydrogel, a disc (8 mm diameter, 1.5 mm thickness) was punched from a hydrogel sheet with a die. A Nile Red solution was prepared as follows: 75 μL of a Nile Red solution (20 mg per mL of methanol) was dissolved in 8 mL of DI water and combined with 120 mL of PBS. Each hydrogel disc was sequentially soaked for 24 h in 60 mL of the aforementioned Nile Red solution and then soaked for 3 days in 60 mL of PBS (exchanged daily). With each disc placed on a glass microscope slide and DI water dropped onto the disc to maintain hydration, images were captured with CLSM using a Leica TCS SP5 confocal microscope (Leica Microsystems, Bannockburn, IL; excitation filter of 488 nm and emission filter 490-570 nm). Images were obtained from 3 μm sections in the z-direction. Images were assigned green for contrast.

2.8. Equilibrium Swelling

Three discs (13 mm diameter) were punched from a single hydrogel sheet with a die. Each disc was placed in a sealed vial containing 20 mL DI water and placed on a rocker table (250 rpm) for 48 hr at RT. Discs were then removed, blotted with filter paper to remove surface water, and weighed (W_s). Equilibrium swelling ratio (SR) is defined as: $SR = (W_s - W_d)/W_d$, where W_s is the weight of the water-swollen hydrogel and W_d is the weight of the vacuum dried hydrogel (30 in. Hg, 60 ºC, 24 hr).

2.9. Dynamic Mechanical Analysis (DMA)

Three discs (13 mm diameter) were prepared as above. Storage modulus (G') of each disc was measured in the compression mode with a dynamic mechanical analyzer (TA Instruments Q800) equipped with parallel-plate compression clamp with a diameter of 40 mm (bottom) and 15 mm (top). A water-swollen disc (13 mm diameter) was blotted with a Kim Wipe, clamped between the parallel plates and silicone oil placed around the exposed hydrogel edge to prevent dehydration. Following equilibration at 25 °C (5 min), the samples were tested in a multi-frequency-strain mode (1 to 25 Hz).

2.10. Degradation

Six hydrogel discs (8 mm diameter) were prepared as above. After soaking in DI water for 3 hr, an initial swollen weight (W_s) was recorded. Three discs were each placed into a well of a 24-well plate containing 1 mL 0.05M NaOH, the well plate covered with Parafilm and foil and maintained at 37 ºC on a rocker table at 50 rpm. The NaOH solution was exchanged every 12 hr. Swollen weights (W_s) were recorded at regular intervals until the hydrogel exhibited an increase in swelling with a corresponding loss in mechanical integrity. The time required for the disc to completely dissolve was also recorded. The remaining three hydrogel discs were vacuum dried (30 in. Hg, 60 ºC, 24 hr) and their weights recorded (W_d). Swelling ratio (SR) is defined as: $SR = (W_s - W_d)/W_d$.

2.11. Bioactivity

2.11.1. Hydrogel Preparation—A hydrogel sheet with 0:100 and 10:90 wt% $PDMS_{star}$-MA to PEG-DA (6 k g/mol) was prepared via SIPS as above. A disc (13 mm diameter) was punched from each sheet and each disc placed into a sealed centrifuge tube containing 40 mL of 1.5X simulated body fluid (SBF)[68] at 37 °C. After two weeks, the hydrogel discs were removed and prepared for SEM imaging as above.

2.11.2. X-ray Diffraction Spectroscopy—Powder X-ray diffraction data was collected on a Bruker D8 diffractometer fitted with LynxEYE detector (CuKa; 40kV, 40 mA; Bragg Brentano geometry; scan range: 5 - 70 degrees; step size: 0.05 degrees; step time: 1 s).

2.12. Nonspecific Protein Adhesion

The adhesion of Alexa Fluor 555 dye conjugate of bovine serum albumin (AF-555 BSA; MW = 66 kDa; Molecular Probes, Inc.) onto hydrogels was studied by fluorescence microscopy. For a given hydrogel, three hydrogel discs (14 mm diameter, 1.5 mm thickness) were punched from a single hydrogel sheet and placed in PBS (15 min) to ensure hydration. Immediately prior to transferring to a 24-well plate, discs were gently blotted with filter paper to remove PBS on the surface. Of the three discs, two discs were each placed in wells containing 1.5 mL of BSA (0.1 mg/mL of PBS) and the third disc was placed in a well containing 1.5 mL of PBS. Hydrogel discs were maintained in the dark at RT for 3 h. Next, from both the top and bottom surfaces of the discs, the BSA solution was carefully removed via aspiration and both sides of the disc were rinsed with fresh PBS 3 times for 1 h each time to permit the diffusion of unadsorbed protein out of the hydrogels before imaging. No

measurable internal fluorescence signal was detected following rinsing. Each of these discs was returned to a well containing 1.5 mL of fresh PBS for imaging.

A Zeiss Axiovert 200 optical microscope equipped with an A-Plan 5X objective (Axiocam HRC Rev. 2), and filter cube (excitation filter of 546 (12 nm [band-pass] and emission filter 575-640 nm [bandpass]) was used to obtain fluorescent images on three randomly selected regions of each hydrogel surface. The fluorescent light source was permitted to warm up for 30 min prior to image capture. Linear operation of the camera was ensured and constant exposure time used during the image collection to permit quantitative analyses of the observed fluorescent signals. The fluorescence microscopy images were analyzed using ImageJ, which yielded the mean and standard deviation of the fluorescence intensity within a given image. For a given hydrogel composition, the average fluorescence intensity of the two discs exposed to AF-555 BSA was subtracted from that of the disc maintained only in PBS to ensure correction for of any fluorescence signal from the material itself. The background corrected fluorescence intensities for each hydrogel were then used to quantify AF-555 BSA levels adsorbed by comparison against a calibration curve constructed from the measured fluorescence intensities of AF-555 BSA standard solutions. Standard solutions were prepared at 0, 0.005, 0.01, 0.02, and 0.04 mg/mL AF-555 BSA in PBS and each placed into an individual well.

2.13. Controlled Introduction of Cell Adhesion and Spreading

Hydrogel sheets were prepared with and without acrylate-derivatized cell-adhesive peptide RGDS in the DCM precursor solutions. RGDS-modified hydrogel sheets (50 × 40 × 1 mm) were fabricated at different wt% ratios of $PDMS_{star}$-MA to PEG-DA (3.4k g/mol) [0:100, 1:99, 10:90 and 20:80] via SIPS as above but with 1 μmol/mL (post-swelling) of acrylate-derivatized RGDS in the DCM precursor solutions. Acryloyl-PEG-RGDS was prepared by reacting acryloyl-PEG-SVA (3.4 kDa) with RGDS.[69] A PEG-DA hydrogel fabricated in water (“PEG Control”) was similarly formed with acrylate-derivatized RGDS from an aqueous precursor solution. The DCM-based sheets were first air dried for 24 hr. Both the water-based and dried DCM-based sheets were sterilized with two changes of ethanol/water (70/30; 24 h) and transferred into sterile Petri dishes where they were washed twice with sterile DI water (24 hr) and finally rinsed twice with Dulbecco’s PBS (pH = 7.2) supplemented with 1% PSA (24 hr). Four (8 mm diameter) discs were punched from each sample and transferred into a 48 well plate. 10T ½ cells were seeded onto the hydrogel surfaces at 10,000 cells/cm^2. After being maintained for 24 hr at 37 °C with 5% CO_2 in DMEM (without phenol red) supplemented with 10% heat-inactivated FBS and 1% PSG, cell adhesion and spreading was examined at 24 h using a bright field microscopy (Zeiss Axiovert).

2.14. Cytocompatibility

Hydrogel sheets prepared for cell adhesion and spreading studies were likewise prepared for cytocompatiblity tests. Hydrogel cytocompatiblity was assessed by measuring lactate dehydrogenase (LDH) levels released by 10T ½ cells 24 hr following cell seeding. Following the aforementioned sterilization protocol, four 8 mm hydrogel discs per sample type were transferred to separate wells of a 48 well plate. Harvested 10T ½ cells were

seeded onto the hydrogel surfaces at 6000 cells/cm^2. After being maintained for 24 hr at 37 °C as above, the media surrounding each specimen was collected for LDH measurements following manufacturer (Roche) protocol.

3. Results and Discussion

3.1. Hydrogel Fabrication

Fig. 1 shows the appearance of precursor solutions and the corresponding hydrogel. As was previously observed,[64] pure PEG-DA hydrogels fabricated via SIPS were similarly transparent compared to the corresponding PEG-DA hydrogel (i.e. fabricated from an aqueous precursor solution). Aqueous precursor solutions became hazy upon addition of hydrophobic PDMS$_{star}$-MA due to its water-insolubility [62] (Fig. 1). Due to the improved solubility of PDMS$_{star}$-MA in DCM, precursor solutions were less hazy and the corresponding hydrogels were not as opaque. To validate photocrosslinking efficacy, hydrogel sol contents were measured. Sol content values of PDMS$_{star}$-PEG hydrogels fabricated from DCM precursor solutions (~2-11%) and aqueous precursor solutions (~0.5-8%) were similarly low (Supplemental Table S1).

3.2. Morphology and Distribution of PDMS

Recently, we prepared macroporous PEG-DA hydrogels via SIPS by employing a DCM precursor solution.[64] During SIPS, macropores are produced by the separation of the growing polymer chains and network from the solvent into polymer rich and polymer lean domains (i.e. pores) that subsequently fill with water during hydration. Because pure PEG-DA hydrogels formed via SIPS did not significantly collapse during prior freeze-drying, their morphology could be examined by SEM.[64] However, SEM images of PDMS$_{star}$-PEG hydrogels revealed that they had significantly collapsed (Supplemental Fig. S1). Thus, the porosity as well as PDMS$_{star}$-MA distribution of hydrated hydrogels was characterized with CLSM (Fig. 2). Regions of the hydrogels containing the hydrophobic PDMS$_{star}$-MA were stained by the hydrophobic dye whereas water-filled pores were unstained. With increased levels of PDMS$_{star}$-MA, hydrogel pore size increased and became macroporous at wt% ratios ≥ 10 wt%. Furthermore, the PDMS$_{star}$-MA is more uniformly distributed versus analogous PDMS$_{star}$-PEG hydrogels fabricated from an aqueous precursor solution in which discrete PDMS-enriched microparticles were observed.[62] Thus, SIPS is useful to achieve macroporous morphologies as well as a more uniform distribution of PDMS.

3.3. Equilibrium Swelling

Swelling of PDMS$_{star}$-PEG hydrogels formed via SIPS was lower than that of the corresponding PDMS$_{star}$-PEG hydrogels produced from aqueous precursor solutions (Table 1, Fig. 3). For “water fabricated” PDMS$_{star}$-PEG hydrogels, PDMS$_{star}$-MA content did not substantially alter hydration, likely due to the discrete nature of the PDMS-enriched microparticles. Hydrophobic PDMS$_{star}$-MA is more soluble in DCM versus water and so becomes more evenly distributed throughout the hydrogels prepared via SIPS (Fig. 2). As a result, increased PDMS$_{star}$-MA content produced a systematic decrease in swelling. While the macroporous nature of PDMS$_{star}$-PEG hydrogels formed via SIPS is expected to increase swelling.[47, 65] PEG-DA hydrogels prepared via SIPS likewise did not exhibit enhanced

swelling versus PEG-DA hydrogels fabricated from aqueous precursor solutions [64] which may be due to reduced swelling of polymer-rich region. Thus, the distribution of water rather than total water uptake is changed by using SIPS to form $PDMS_{star}$-PEG hydrogels.

3.4. Modulus

Hydrogel stiffness was quantified in term of the compressive storage modulus (G') obtained by DMA (Fig. 4). As previously reported for PED-DA hydrogels,[31, 70] G' of $PDMS_{star}$PEG hydrogels prepared via SIPS increased with higher crosslink density (i.e. lower PEG-DA M_n). G' was substantially higher for hydrogels fabricated via SIPS compared to the corresponding hydrogels fabricated from aqueous precursor solutions. There are two contributing factors to this observation. First, for a given composition, $PDMS_{star}$-PEG hydrogels prepared via SIPS exhibited reduced swelling (Fig. 3) which is typically associated with enhanced rigidity.[27] Second is the effect of the macroporous morphology of the hydrogels prepared via SIPS (Fig. 2). Indeed, despite minor changes in swelling, pure PEG-DA hydrogels prepared via SIPS were macroporous and exhibited a pronounced increase in G' versus when fabricated in water.[64] For hydrogels formed via SIPS, the associated thicker pore walls may be the source of the increase in G'.

3.5 Degradation

Hydrolytic degradation of $PDMS_{star}$-PEG hydrogels was measured under accelerated (basic) conditions (Fig. 5). Degradation was quantified in terms of the time to reach maximum swelling before loss of mechanical integrity as well as the time for complete dissolution.[58] For aliphatic polyesters, the rate of hydrolytic degradation increases with larger pore size and hence greater pore wall thickness [17] as well as film thickness [71] due to an autocatalytic effect of more slowly diffusing acidic degradation products. Under basic conditions, macroporous PEG-DA hydrogels formed via SIPS likewise degraded faster than the corresponding hydrogel fabricated from aqueous precursor solutions.[64] For PEG-DA-based hydrogels, hydrolysis of ester bonds releases poly(acrylic acid) (PAA) kinetic chains [72] capable of inducing autoacceleration if diffusion is limited. However, under basic conditions, the increased degradation rate may be largely attributed to the limited diffusion of hydroxide ions through thicker pore walls which proceed to catalyze bond cleavage. Likewise, the observed increased degradation rate of $PDMS_{star}$-PEG hydrogels fabricated via SIPS versus the corresponding hydrogel fabricated in water is attributed to the former's increased pore size and thicker pore walls. As expected, degradation rate increased for hydrogels prepared with 6k g/mol PEG-DA versus from 3.4k g/mol PEG-DA due to the former's lower crosslink density. The effect of M_n was similarly observed for $PDMS_{star}$-PEG hydrogels fabricated from aqueous precursor solutions (Supplemental Fig. S2). Incorporation of $PDMS_{star}$-MA into hydrogels formed via SIPS led to an increased degradation time but did not necessarily coincide with $PDMS_{star}$-MA content. For these hydrogels, as $PDMS_{star}$-MA content increases, the degradation rate is influenced by both the increased hydrophobicity that reduces degradation [73] and the increased pore size that enhances degradation. Given the limited susceptibility to hydrolysis of PEG-DA-based hydrogels, their fabrication by SIPS to produce enhanced degradation rates as well as the ability to further increase degradation rates through the incorporation of $PDMS_{star}$-MA

provide useful mechanisms to enhance the utility of PEG-DA hydrogels for tissue engineering.

3.6. Bioactivity - Hydroxyapatite Formation

Bioactive materials chemically bond to bone via formation of a biological active hydroxyapatite (HAp) layer.[74] Calcium apatites such as HAp have also been shown to promote differentiation of mesenchymal stem cells (MSCs) to osteoblasts (i.e. are osteoinductive).[75] Since inorganic, hydrophobic materials are associated with bioactivity [20-22], we anticipated that $PDMS_{star}$-PEG hydrogels prepared via SIPS would be bioactive. The degree of formation of HAp upon immersion into SBF is a qualitative indication of the level of scaffold bioactivity and has been correlated to the ability to bond to bone *in vivo*. [76] Thus, the extent of formation of HAp following SBF exposure was compared for a $PDMS_{star}$-PEG (3.4k g/mol) hydrogel (10:90 wt% ratio) versus the pure PEG-DA (3.4k g/mol) control (i.e. no PDMS) and $PDMS_{star}$-PEG (6k g/mol) hydrogel (20:80 wt% ratio) versus the pure PEG-DA (6k g/mol) control (i.e. no PDMS) (Fig. 6). SEM images revealed a significant level of HAp on the $PDMS_{star}$-PEG hydrogel but its absence on the PEG-DA hydrogel. X-ray diffraction was performed on these hydrogel compositions to verify HAp formation and characteristic HAp peaks of 31.7, 45.5, and 56.5 were noted. These peaks indicate reflections from 112, 222, 004 crystal planes respectively and correspond to Bragg reflections of HAp (Fig. 7).[77] In our previous study, $PDMS_{star}$-PEG hydrogels prepared from aqueous precursor solutions demonstrated increased stimulation of osteogenic differentiation of encapsulated MSCs.[63] On the basis of these studies, $PDMS_{star}$-PEG hydrogels prepared via SIPS are bioactive and may increase the osteogenic potential of associated MSCs.

3.7. Nonspecific Protein Adhesion

Because cell behavior is altered by adsorbed proteins (e.g. from serum),[37, 78] scaffolds useful to study materials-guided cell behavior must be significantly protein resistant. The adsorption of BSA onto $PDMS_{star}$-PEG hydrogels prepared via SIPS was compared to that of the corresponding PEG-DA hydrogels (Table 1). BSA adsorption on PEG-DA hydrogels has been shown to increase with reduced hydration.[79] As noted above, swelling was reduced with increased $PDMS_{star}$-MA content for $PDMS_{star}$-PEG hydrogels prepared via SIPS. When based on 6k g/mol PEG-DA, $PDMS_{star}$-PEG hydrogels formed via SIPS exhibited somewhat similar BSA adsorption versus the pure PEG-DA control. BSA adsorption was somewhat higher for hydrogels based on 3.4k g/mol PEG-DA versus the PEG-DA control. This may be due to the lower hydration of hydrogels based on 3.4k g/mol versus 6k g/mol PEG-DA. However, for all $PDMS_{star}$-MA:PEG-DA hydrogels, protein adsorption levels were within the range reported for PEG-DA hydrogels.[79] Furthermore, BSA adsorption was similar for $PDMS_{star}$-PEG hydrogels prepared by SIPS versus that of analogous hydrogels prepared in water, despite the former's reduced swelling. The increased pore size of $PDMS_{star}$-PEG hydrogels prepared by SIPS may enhance protein diffusion thereby reducing its adsorption.

3.8. Controlled Introduction of Cell Adhesion and Spreading

PEG-DA hydrogels' resistance to adsorption of bioactive serum proteins renders them "biological blank slates" as cells are subsequently unable to adhere and spread.[35] Defined levels of cell adhesion may be introduced by covalent incorporation of acrylate-functionalized cell adhesive peptide RGDS into PEG hydrogels.[36, 80-81] While we observed minor changes in protein adsorption, maintenance of the biological blank slate nature for $PDMS_{star}$-PEG hydrogels was assessed by evaluating cell adhesion onto hydrogels prepared with and without acrylate-RGDS (Fig. 8). $PDMS_{star}$PEG hydrogels based on 3.4k g/mol PEG-DA were prepared via SIPS both with and without 1 μmol/mL of acrylate-derivatized RGDS. A PEG-DA hydrogel fabricated in water similarly prepared with and without RGDS served as a control ("PEG Control"). Incorporation of low levels of RGDS has been observed to cause only a minute change in hydrogel swelling.[82] As with the PEG control, cells did not adhere and spread in the absence of RGDS. However, modification of all hydrogels with RGDS did cause cell adhesion and spreading. Thus, as for "water fabricated" PEG-DA hydrogels, $PDMS_{star}$-PEG hydrogels prepared via SIPS permit the controlled introduction of cell adhesion and spreading which is critical for their utility to study cell-material interactions.

3.9. Cytocompatibility

Low cytotoxicity of $PDMS_{star}$-PEG hydrogels prepared via SIPS is essential for their utility as tissue engineering scaffolds. Cytocompatiblity was assessed by measuring LDH levels released by 10T½ cells 24 hr post-seeding onto RGDS-modified hydrogels based on 3.4k g/mol PEG-DA as a representative series (Fig. 9). LDH is a soluble cytosolic enzyme that is released into the culture medium following membrane damage due to apoptosis or necrosis.[83] Thus, differences in the normalized levels of exogenous LDH across cell-laden hydrogels are indicative of the amount of cell death induced by the hydrogel composition. At all levels of $PDMS_{star}$-MA, the relative LDH activity associated with $PDMS_{star}$-PEG hydrogels prepared via SIPS were similar to pure PEG-DA hydrogels prepared via SIPS as well as PEG-DA hydrogels fabricated from aqueous precursor solutions. Thus, at these levels of $PDMS_{star}$-MA, $PDMS_{star}$-PEG hydrogels maintain the low cytotoxicity of PEG-DA hydrogels.

4. Conclusions

Hydrogels which maintain the useful properties of PEG-DA hydrogels but extend their physical and chemical properties would be useful for controlled cell-material interaction studies. In this study, $PDMS_{star}$-PEG hydrogels were fabricated via SIPS to produce macroporous morphologies and a more even distribution of bioactive PDMS versus when fabricated from an aqueous precursor solution. Hydrogel properties were tuned by adjusting the wt% ratio of $PDMS_{star}$-MA:PEG-DA (0:100, 1:99, 10:90 an 20:80) as well as PEG-DA M_n (3.4k or 6k g/mol). A pronounced increase in hydrogel stiffness (G') was observed for $PDMS_{star}$-PEG hydrogels fabricated via SIPS versus the corresponding hydrogel fabricated from an aqueous precursor solution and was shown to increase with $PDMS_{star}$-MA content. In addition, the degradation rate was enhanced for hydrogels formed via SIPS. While PEG-DA hydrogels did not demonstrate bioactivity (i.e. formation of HAp upon submersion into

SBF), $PDMS_{star}$-PEG hydrogels fabricated via SIPS were bioactive. This is attributed to the hydrophobic, inorganic nature of the PDMS. SIPS-produced $PDMS_{star}$-PEG hydrogels did substantially adsorb higher levels of BSA versus a PEG-DA hydrogel fabricated in water. As a result, cell adhesion and spreading onto $PDMS_{star}$-PEG hydrogels was observed only on hydrogels modified with the cell adhesive peptide RGDS. Thus, these $PDMS_{star}$-PEG hydrogels maintain the biological blank slate nature of "water fabricated" PEG-DA hydrogels. Thus, these new $PDMS_{star}$-PEG hydrogels formed by SIPS are useful to use, along with pure PEG-DA and $PDMS_{star}$-PEG hydrogels formed from aqueous precursor solutions, to study materials-guided cell behavior and tissue regeneration.

Supplementary Material

Refer to Web version on PubMed Central for supplementary material.

Acknowledgments

Funding from the NIH/NHLBI (1R21HL089964) is gratefully acknowledged.

References

[1]. Dutta RC, Dutta AK. Cell-interactive 3D-scaffold; advances and applications. Biotech Adv. 2009;27:334–9.

[2]. Kleinman HK, Philp D, Hoffman MP. The role of the extracellular matrix in morphogenesis. Curr Opin Biotechnol. 2003;14:526–32. [PubMed: 14580584]

[3]. Lutolf MP, Hubbell JA. Synthetic biomaterials as instructive extracellular microenvironments for morphogensis in tissue engineering. Nature Biotech. 2005;23:47–55.

[4]. Brandl F, Sommer F, Goepferich A. Rational design of hydrogels for tissue engineering: Impact of physical factors on cell behavior. Biomaterials. 2007;28:134–6. [PubMed: 17011028]

[5]. Pennesi C, Scaglione S, Gionnoni P, Quarto R. Regulatory influence of scaffolds on cell behavior: How cells decode biomaterials. Curr Pharm Biotech. 2011;12:151–9.

[6]. Liao H, Munoz-Pinto D, Qu X, Hou Y, Grunlan MA, Hahn MS. Influence of hydrogel mechanical properties and mesh size on vocal fold fibroblast extracellular matrix production and phenotype. Acta Biomater. 2008;4:1161–71. [PubMed: 18515199]

[7]. Engler AJ, Sen S, Sweeney HL, Discher DE. Matrix elasticity directs stem cell lineage specification. Cell. 2006;126:677–89. [PubMed: 16923388]

[8]. Discher DE, Janmey P, Wang Y-l. Tissue cells feel and respond to the stiffness of their substrate. Science. 2005;310:1139–43. [PubMed: 16293750]

[9]. Dado D, Levenberg S. Cell-scaffold mechanical interplay within engineered tissues. Sem Cell Dev Biol. 2009;20:656–64.

[10]. Crouch AS, Miller D, Luebke KJ, Hu W. Correlation of anisotropic cell behaviors with topographic aspect ratio. Biomaterials. 2009;30:1560–7. [PubMed: 19118891]

[11]. Glawe JD, Hill JB, Mills DK, McShane MJ. Influence of channel width on alignment of smooth muscle cells by high-aspect-ratio microfabricated elastomeric cell culture scaffolds. J Biomed Mater Res. 2005;75A:106–14.

[12]. Nichol JW, Khademhosseini A. Modular tissue engineering: Engineering biological tissues from the bottom up. Soft Matter. 2009;5:1312. [PubMed: 20179781]

[13]. Khetan S, Burdick JA. Patterning hydrogels in three dimensions towards controlling cellular interactions. Soft Matter. 2011;7:830–8.

[14]. McGlohorn JB, Holder WDJ, Grimes LW, Thomas CB, Burg KJL. Evaluation of smooth muscle cell response using two types of porous polylactide scaffolds with differing pore topography. Tissue Eng. 2004;10:505–14. [PubMed: 15165467]

[15]. Khademhosseini A, Langer R. Microengineered hydrogels for tissue engineering. Biomaterials. 2007;28:5087. [PubMed: 17707502]

[16]. Woodfield TBF, Moroni L, Malda J. Combinatorial approaches to controlling cellular interactions. Soft Matter. 2009;12:562–79.

[17]. Odelius K, Hoeglund A, Kumar S, Hakkarainen M, Ghosh AK, Bhatnagar N. Porosity and pore size regulate the degradation product profile of polylactide. Biomacromolecules. 2011;12:1250–8. [PubMed: 21344847]

[18]. Keskar V, Marion NW, Mao JM, Gemeinhart RA. *In vitro* evaluation of macroporous hydrogels to facilitate stem cell infliltration, growth, and mineralization. Tissue Eng A. 2009;15:1695–707.

[19]. Wu L, Ding J. Effects of porosity and pore size on *in vitro* degradation of three-dimensional porous poly(D,L-lactide-*co*-glycolide) scaffolds for tissue engineering. J Biomed Mater Res. 2005;75A:767–77.

[20]. Ning CQ, Mehta J, El-Ghannam A. Effect of silica on the bioactivity of calcium phosphate composites *in vitro*. J Mater Sci Mater Med. 2005;16:355–60. [PubMed: 15803281]

[21]. Song J-H, Yoon B-H, Kim Y-E, Kim H-W. Bioactive and degradable hybridized nanofibers of gelatin-siloxane for bone regeneration. J Biomed Mater Res. 2008;84:875–84.

[22]. Ren L, Tsuru K, Hayakawa S, Osaka A. Novel approach to fabricate porous gelatin-siloxane hybrids for bone tissue engineering. Biomaterials. 2002;23:4765–73. [PubMed: 12361615]

[23]. Benoit DSW, Schwartz MP, Durney AR, Anseth KS. Small functional groups for controlled differentiation of hydrogel-encapsulated human mesenchymal stem cells. Nat Mater. 2008;7:816–23. [PubMed: 18724374]

[24]. Escobar-Ivirico JL, Salmeron-Sanchez M, Gomez-Ribelles JL, Monleon-Pradas M, Soria JM, Gomes ME, et al. Proliferation and differentiation of goat bone marrow stromal cells in 3D scaffolds with tunable hydrophilicity. J Biomed Mater Res. 2009;91B:277–86.

[25]. Ayala R, Zhang C, Yang D, Hwang Y, Aung A, Shroff SS, et al. Engineering the cell-material interface for controlling stem cell adhesion, migration, and differentiation. Biomaterials. 2011;32:3700–11. [PubMed: 21396708]

[26]. Jansen EJP, Sladek REJ, Bahar H, Yaffe A, Gijbels MJ, Kuijer R, et al. Hydrophobicity as a design criterion for polymer scaffolds in bone tissue engineering. Biomaterials. 2005;26:4423–31. [PubMed: 15701371]

[27]. Anseth KS, Bowman CN, Brannon-Peppas L. Mechanical properties of hydrogels and their experimental determination. Biomaterials. 1996;17:1647–57. [PubMed: 8866026]

[28]. Burdick JA, Anseth KS. Photoencapsulation of osteoblasts in injectable RGD-modified PEG hydrogels for bone tissue engineering. Biomaterials. 2002;23:4315–23. [PubMed: 12219821]

[29]. Yang F, Williams CG, Wang D-A, Lee H, Manson PN, Elisseef J. The effect of incorporating RGD adhesive peptide in polyethylene glycol diacrylate hydrogel on osteogenesis of bone marrow stromal cells. Biomaterials. 2005;26:5991–8. [PubMed: 15878198]

[30]. Paxton JZ, Donnelly K, Keatch RP, Baar K. Engineering the bone-ligament interface using polyethylene glycol diacrylate incorporated with hydroxyapatite. Tissue Eng. 2009;15:1201–9.

[31]. Bryant SJ, Anseth KS. Hydrogel properties influence ECM production by chondrocytes photoencapsulated in poly(ethylene glycol) hydrogels. J Biomed Mater Res. 2002;59:63–72. [PubMed: 11745538]

[32]. Bryant SJ, Nicodemus GD, Vallanueva I. Designing 3D photopolymer hydrogels to regulate biomechanical cues and tissue growth for cartilage tissue engineering. Pharm Res. 2008;25:2379–86. [PubMed: 18509600]

[33]. Hahn MS, McHale MK, Wang E, Schmedlen RH, West JL. Physiological pulsatile flow bioreactor conditioning of poly(ethylene glycol)-based tissue engineering grafts. Ann Biomed Eng. 2007;35:190–200. [PubMed: 17180465]

[34]. Mahoney MJ, Anseth KS. Three-dimensional growth and function of neural tissue in degradable polyethylene glycol hydrogels. Biomaterials. 2006;27:2265–74. [PubMed: 16318872]

[35]. Gombotz WR, Guanghui W, Horbett TA, Hoffman AS. Protein adsorption to poly(ethylene oxide) surfaces. J Biomed Mater Res. 1991;25:1547–62. [PubMed: 1839026]

[36]. Hahn MS, Miller JS, West JL. Three-dimensional biochemical and biomechanical patterning for guiding cell behavior. Adv Mater. 2006;18:2679–84.

[37]. Mann BK, Gobin AS, Tsai AT, Schmedlen RH, West JL. Smooth muscle cell growth in photopolymerized hydrogels with cell adhesive and proteolytically degradable domains: Synthetic ECM analogs for tissue engineering. Biomaterials. 2001;22:3045–51. [PubMed: 11575479]

[38]. Zhang H, Wang L, Song L, Niu G, Cao H, Wang G, et al. Controllable properties and microstructure of hydrogels based on crosslinked poly(ethylene glycol) diacrylates with different molecular weights. J Appl Polym Sci. 2011;121:531–40.

[39]. Munoz-Pinto D, Bulick AS, Hahn MS. Uncoupled investigation of scaffold modulus and mesh size on smooth muscle cell behavoir J Biomed Mater Res. 2009;90A:303–16.

[40]. Gudipati CFG, Greenlief CM, Johnson JA, Prayongpan P, Wooley KL. Hyperbranched fluoropolymer (HBFP) and linear poly(ethylene glycol) (PEG) based on amphiphilic crosslinked networks as efficeint anti-fouling coatings: An insight into the surface compositions, topographies and morphologies. J Polym Sci Part A: Polym Chem. 2004;42:6193–208.

[41]. McGlohorn JB, Holder J, Grimes LW, Thomas CB, Burg KJL. Evaluation of smooth muscle cell response using two types of porous polylactide scaffolds with differing pore topography. Tissue Eng. 2004;10:505–14. [PubMed: 15165467]

[42]. Sarkar S, Dadhania M, Rourke P, Desai TA, Wong JY. Vascular tissue engineering: microtextured scaffold templates to control organization of vascular smooth muscle cells and extracellular matrix. Acta Biomater. 2005;1:93–100. [PubMed: 16701783]

[43]. Ford MC, Bertram JP, Hynes SR, Michaud M, Li Q, Young M, et al. A macroporous hydrogel for the coculture of neural progenitor and endothelial cells to form functional vascular networks *in vivo*. Proc Nat Acad Sci. 2006;103:2512–7. [PubMed: 16473951]

[44]. Yoon DM, Fisher JP. Chondrocyte signaling and artificial matrices for articular cartilage engineering. Adv Exp Med Biol. 2006;585:67–86. [PubMed: 17120777]

[45]. Lin S, Sangaj N, Razafiarison T, Zhang C, Varghese S. Influence of physical properties of biomaterials on cellular behavior. Pharm Res. 2011;28:1422–30. [PubMed: 21331474]

[46]. Chen C-W, Betz MW, Fisher JP, Paek A, Chen Y. Macroporous hydrogel scaffolds and their characterization by optical coherence tomography. Tissue Eng C. 2011;17:101–12.

[47]. Chiu Y-C, Larson JC, Isom AJ, Brey EM. Generation of porous poly(ethylene glycol) hydrogels by salt leaching. Tissue Eng Part C. 2010;16:905–12.

[48]. Sannino A, Netti PA, Madaghiele V, Coccoli V, Luciani A, Maffezzoli A, et al. Synthesis and characterization of macroporous poly(ethylene glycol)-based hydrogels for tissue engineering application. J Biomed Mater Res A. 2006:229–36. [PubMed: 16752396]

[49]. Hwang Y, Sangaj N, Varghese S. Interconnected macroporous poly(ethylene glycol) cryogels as a cell scaffold for cartilage tissue engineering. Tissue Eng A. 2010;16:3033–41.

[50]. Hwang Y, Zhang C, Varghese S. Poly(ethylene glycol) cryogels as potential cell scaffolds: Effect of polymerization conditions on cryogel microstructure and properties. J Mater Chem. 2010;20:345–51.

[51]. Annabi N, Nichol JW, Zhong X, Ji C, Koshy S, Khademhosseini A, et al. Controlling porosity and microarchitecture of hydrogels for tissue engineering. Tissue Eng B. 2010;16:371–83.

[52]. Kim B-S, Nikolovski J, Bonadio J, Smiley E, Mooney DJ. Engineered smooth muscle tissues: regulating cell phenotype with the scaffold. Exp Cell Res. 1999;251:321–8.

[53]. Escobar-Ivirico JL, Salmeron-Sanchez M, Gomez-Ribelles JL, Monleon-Pradas M, Soria JM, Gomes ME, et al. Proliferation and differentiation of goat bone marrow stromal cells in 3D scaffolds with tunable hydrophilicity. J Biomed Mater Res. 2009;91B:277–86.

[54]. Lin NJ, Lin-Gibson S. Osteoblast response to dimethacrylate composites varying in composition, conversion and roughness using a combinatorial approach. Biomaterials. 2009;30:4480–7. [PubMed: 19520423]

[55]. Ning CQ, Mehta J, El-Ghannam A. Effect of silica on the bioactivity of calcium phosphate composites *in vitro*. J Mater Sci Mater Med. 2005;16:355–60. [PubMed: 15803281]

[56]. Song J-H, Yoon B-H, Kim Y-E, Kim H-W. Bioactive and degradable hybridized nanofibers of gelatin-siloxane for bone regeneration. J Biomed Mater Res. 2008;84:875.

[57]. McBath RA, Shipp DA. Swelling and degradation of hydrogels synthesized with degradable poly(b-amino ester) crosslinkers. Polym Chem. 2010;1:860–5.

[58]. Metters AT, Anseth KS, Bowman CN. Fundamental studies of a novel, biodegradable PEG-*b*-PLA hydrogel. Polymer. 2000;41:3993–4004.

[59]. West JL, Hubbell JA. Polymeric biomaterials with degradation sites for proteases involved in cell migration. Macromolecules. 1999;32:241–4.

[60]. Gupta G, El-Ghannam A, Kirakodu S, Khraisheh M, Zbib H. Enhancement of osteoblast gene expression by mechanically compatible porous Si-rich nanocomposite. J Biomed Mater Res B. 2007;81:387–96.

[61]. Fisher JP, Lalani Z, Bossano CM, Brey EM, Demian N, Johnston CM, et al. Effect of biomaterial properties on bone healing in a rabbit tooth extration socket model. J Biomed Mater Res Part A. 2004;68:428–38.

[62]. Hou Y, Schoener CA, Regan KR, Munoz-Pinto D, Hahn MS, Grunlan MA. Photo-cross-linked PDMSstar-PEG Hydrogels: Synthesis, characterization, and potential application for tissue engineering scaffolds. Biomacromolecules. 2010;11:648–56. [PubMed: 20146518]

[63]. Munoz-Pinto D, Jimenez-Vergara AC, Hou Y, Hayenga HN, Grunlan MA, Hahn MS. Examination of the osteogenic potential of poly(ethylene glycol)-poly(dimethylsiloxane) hybrid hydrogels. Tissue Eng. 2011; in review.

[64]. Bailey BM, Hui V, Fei R, Grunlan MA. Tuning PEG-DA hydrogel properties via solvent-induced phase separation (SIPS). J Mater Chem. 2011;21:18776–82. [PubMed: 22956857]

[65]. Zhang X-Z, Yang Y-Y, Chung T-S. Effect of mixed solvents on characteristics of poly(*N*-isopropylacrylamide) gels. Langmuir. 2002;18:2538–42.

[66]. Shibayama M, Morimoto M, Nomura S. Phase separation induced mechanical transition of poly(*N*-isopropylacrylamide)/water isochore gels. Macromolecules. 1994;27:5060–6.

[67]. Grunlan MA, Lee NS, Mansfield F, Kus E, Finlay JA, Callow JA, et al. Minimally invasive polymer surfaces prepared from star oligosiloxanes and star oligofluorosiloxanes. J Polym Sci, Part A: Polym Chem. 2006;44.

[68]. Kokubo T, Takadama H. How useful is SBF in predicting in vivo bone bioactivity? Biomaterials. 2006;27:2907–15. [PubMed: 16448693]

[69]. Lynn AD, Kyriakides TR, Bryant SJ. Characterization of the *in vitro* macrophage response and *in vivo* host response to poly(ethylene glycol)-based hydrogels. J Biomed Mater Res. 2010;93A: 941–53.

[70]. Zhang H, Wang L, Song L, Niu G, Cao H, Wang G, et al. Controllable properties and microstructure of hydrogels based on crosslinked poly(ethylene glycol) diacrylates with different molecular weights. J Appl Polym Sci. 2011;121:531–40.

[71]. Lu L, Garcia CA, Mikos AG. *In vitro* degradation of thin poly(DL-lactic-*co*-glycolic acid) films. J Biomed Mat Res. 1999;46:236–44.

[72]. Peters R, Litvinov VM, Steeman P, Dias AA, Mengerink Y, Benthem Rv, et al. Characterisation of UV-cured acrylate networks by means of hydrolysis followed by aqueous size-exclusion combined with reversed-phase chromatography. J Chromatography 2007;11A:111–23.

[73]. Griffith LG. Polymeric biomaterials. Acta Mater. 2000;48:263–77.

[74]. Hench LL. Bioceramics. J Amer Ceram Soc. 1998;81:1705–28.

[75]. Habibovic P, deGroot K. Osteoinductive biomaterials - properties and relavence in bone repair. J Tissue Eng Regen Med. 2007;1:25–32. [PubMed: 18038389]

[76]. Kokubo T, Kushitani H, Sakka S, Kitugi T, Yamanuro T. Solutions able to reporduce in vivo surface-structure changes in bioactive glass-ceramic. J Biomed Mater Res Part A. 1990;24:721–34.

[77]. Liji Sobhana SS, Sundaraseelan J, Sekar S, Sastry TP, Mandal AB. Gelatin-chitosan composite capped gold nanoparticles: a matrix for the growth of hydroxyapatite. J Nanopart Res. 2009;11:333–40.

[78]. Kim BS, Nikolovski J, Bonadio J, Smiley E, Mooney DJ. Engineered smooth muscle tissues: regulating cell phenotype with the scaffold. Exp Cell Res. 1999;251:321–8.

[79]. Ju H, McCloskey BD, Sagle AC, Kusuma VA, Freeman BD. Preparation and characterization of crosslinked poly(ethylene glycol) diacrylate hydrogels as fouling -resistant membrane coatings. J Membr Sci. 2009;330:180–8.

[80]. Yang F, Williams CG, Wang D-A, Lee H, Manson PN, Elisseeff J. The effect of incorporating RGD adhesive peptide in polyethylene glycol diacrylate hydrogel on osteogenesis of bone marrow stromal cells. Biomaterials. 2005;26:5991–8. [PubMed: 15878198]

[81]. Burdick JA, Anseth KS. Photoencapsulation of osteoblasts in injectable RGD-modified PEG hydrogels for bone tissue engineering. Biomaterials 2002;23:4315–23. [PubMed: 12219821]

[82]. Munoz-Pinto DJ, Bulick AS, Hahn MS. Uncoupled investigation of scaffold modulus and mesh size on smooth muscle cell behavior. J Biomed Mater Res Part A. 2009;90A:303–16.

[83]. Renner K, Amberger A, Konwalinka G, Kofler R, Gnaiger E. Changes of mitochondrial respiration, mitochondrial content and cell size after induction of apoptosis in leukemia cells. Biochim Biophys Acta. 2003;1642:115–23. [PubMed: 12972300]

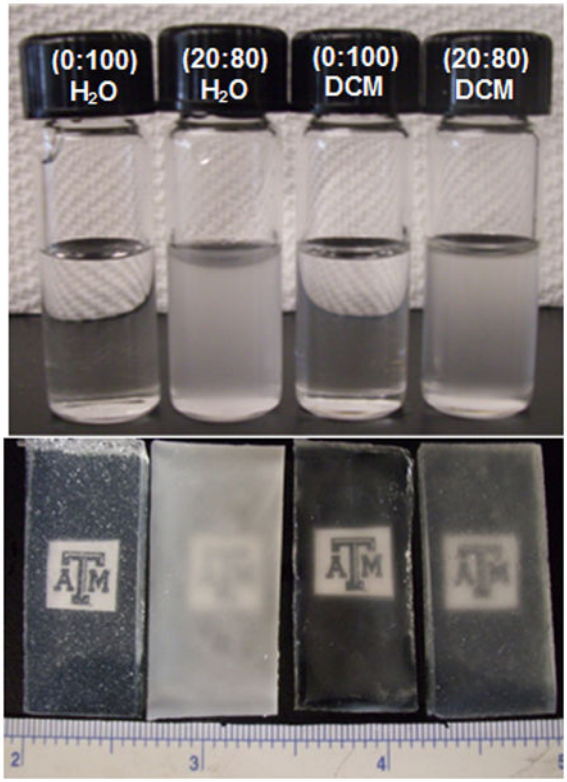

Figure 1.

Precursor solutions **[top]** and corresponding hydrogels **[bottom]** formed from an aqueous precursor solution (left) and *via* SIPS (right) (i.e. with a DCM precursor solution followed by subsequent drying and hydration) with 6k g/mol PEG-DA.

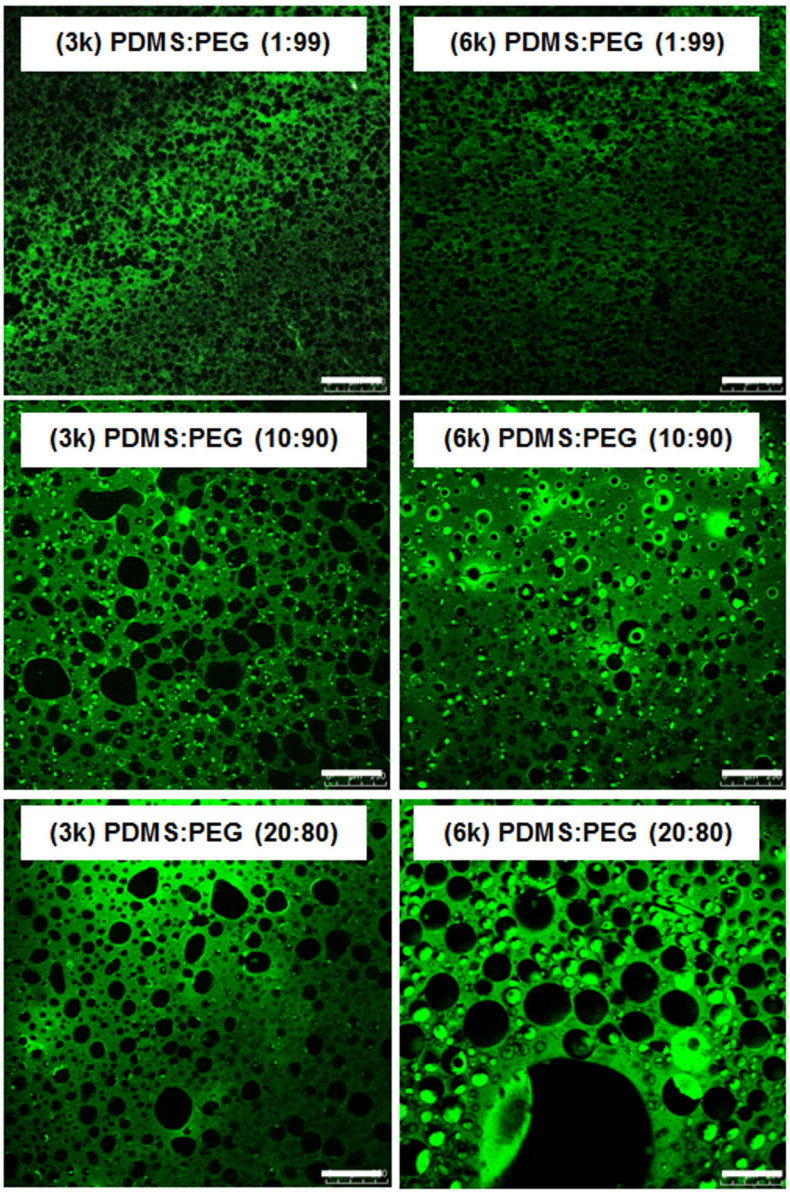

Figure 2.

CLSM images of hydrated $PDMS_{star}$-PEG hydrogels prepared with different wt% ratios of $PDMS_{star}$-MA:PEG-DA from a DCM precursor solution (i.e. *via* SIPS). PDMS-enriched regions stained with hydrophobic dye (Nile Red). (scale bars = 250 μm)

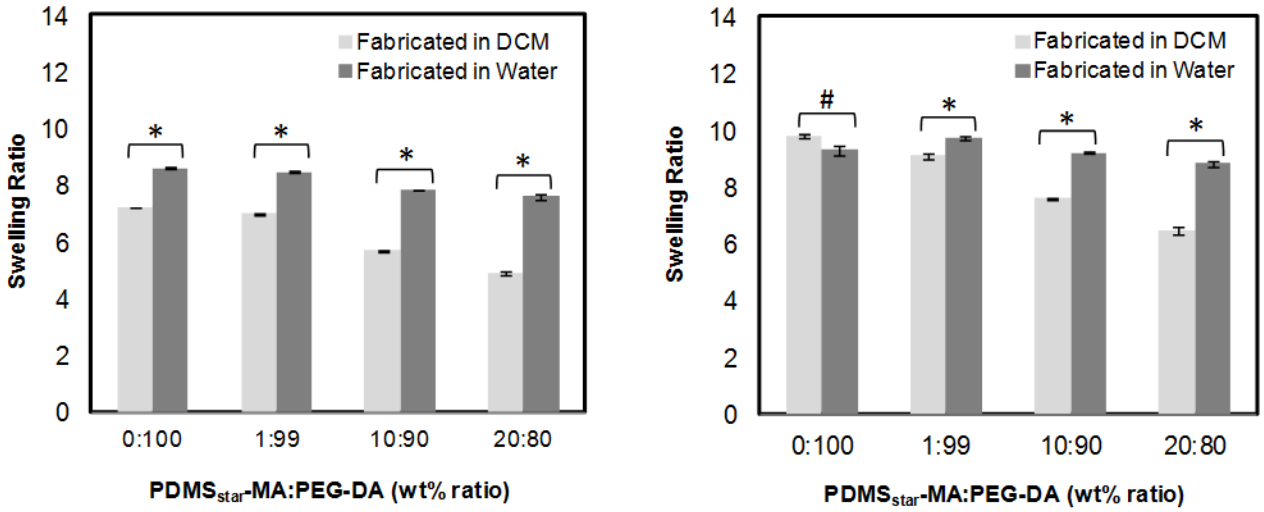

Figure 3.

Swelling ratio of $PDMS_{star}$-PEG hydrogels fabricated with 3.4k g/mol (left) and 6k g/mol (right) PEG-DA from a DCM precursor solution (i.e. *via* SIPS) or from an aqueous precursor solution. Statistical significance was determined by student's *t*-test where (*): $p < 0.05$ and (#): $p > 0.05$.

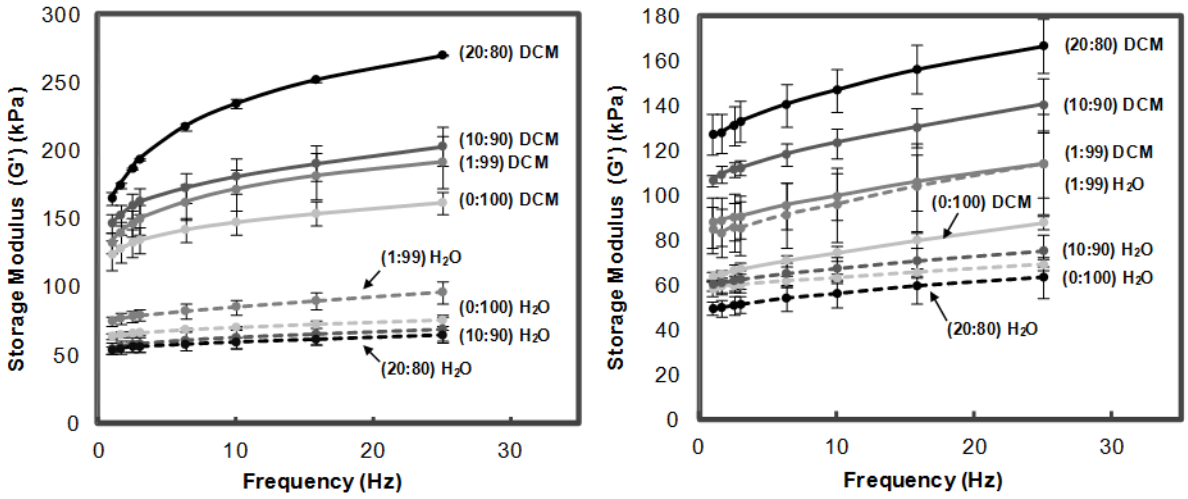

Figure 4.

Storage modulus (G') of $PDMS_{star}$-PEG hydrogels fabricated with PEG-DA 3.4k g/mol (left) and 6k g/mol (right). Hydrogels fabricated from a DCM precursor solution (i.e. *via* SIPS) are denoted with "*solid lines*". Hydrogel or from an aqueous precursor solution are denoted with "*dashed lines*".

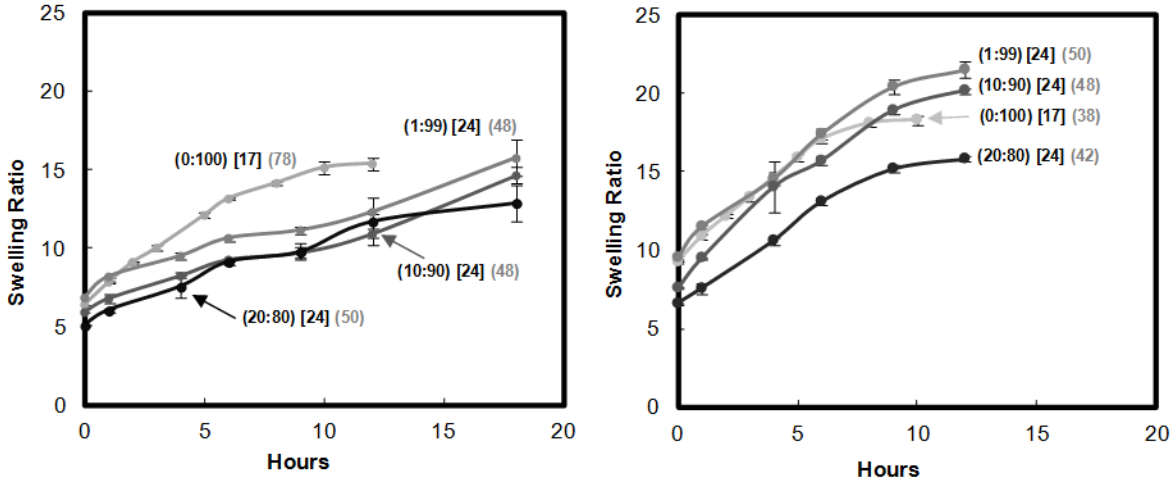

Figure 5.

Swelling ratio under basic conditions (0.05 M NaOH) of $PDMS_{star}$-MA:PEG-DA hydrogels fabricated via SIPS with 3.4k g/mol (left) and 6k g/mol (right) PEG-DA. **[ ]** = hours to complete dissolution and **( )** = hours to complete dissolution of analogous hydrogel (i.e. fabricated from aqueous precursor solutions).

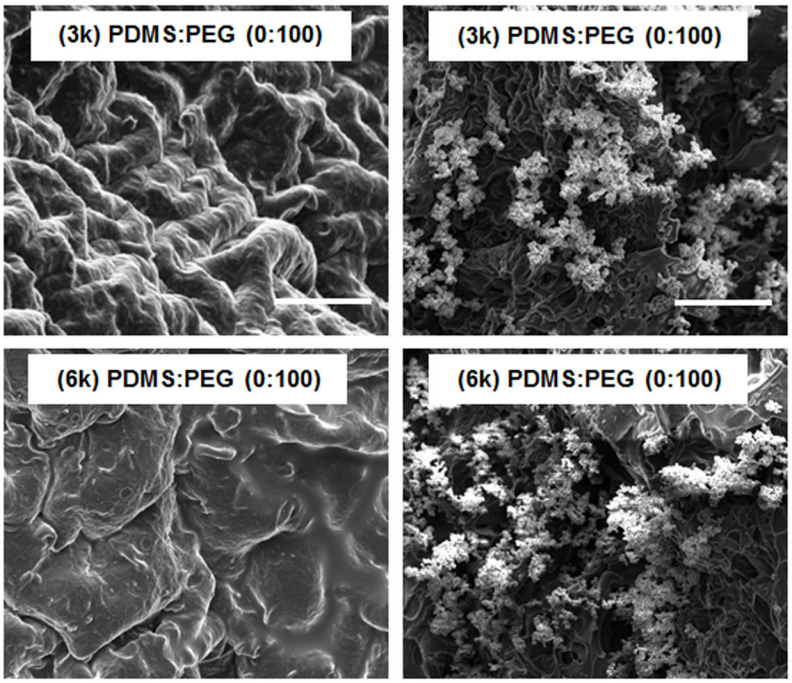

Figure 6.

SEM images (following exposure to SBF for 2 weeks) of hydrogels fabricated with either 3.4k (top) or 6k g/mol (bottom) PEG-DA from a DCM precursor solution (i.e. via SIPS) without PDMS (left column) and with PDMS (right column) and (scale bars = 50 μm).

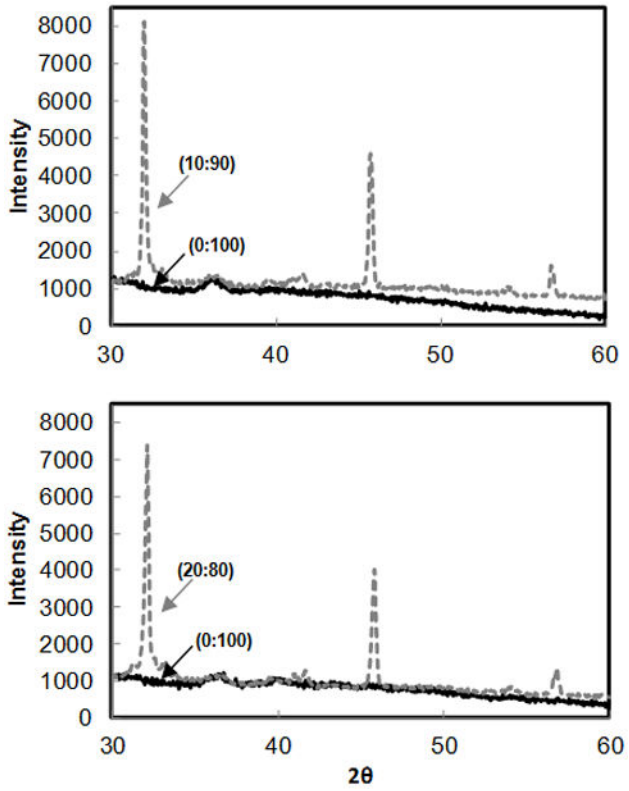

Figure 7.

X-ray Diffraction of PDMS:PEG (3.4k and 6k g/mol) hydrogels soaked in SBF - revealing the formation of HAp within hydrogels when PDMS is incorporated (dotted line) and absence of HAp when no PDMS is incorporated (solid line).

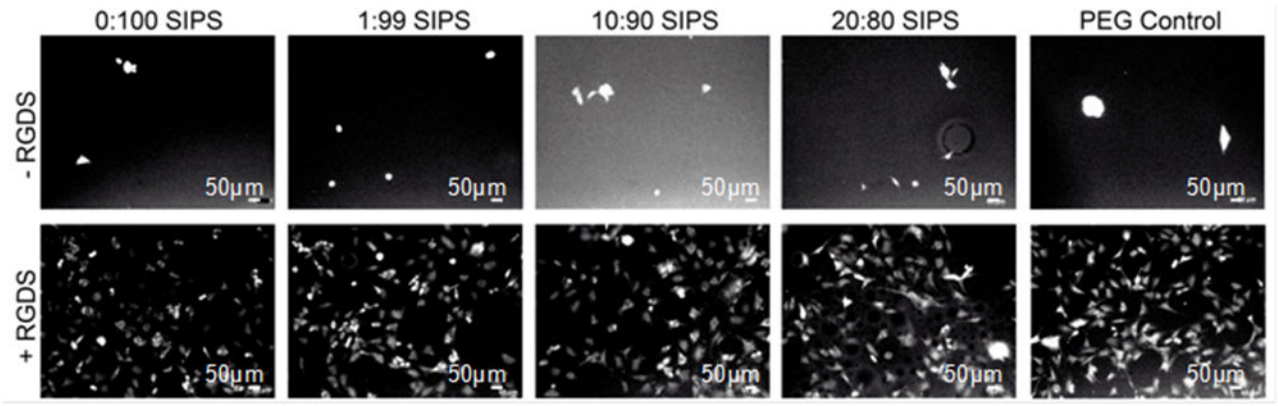

Figure 8.

Cell spreading for $PDMS_{star}$-PEG hydrogels prepared without [top] and with [bottom] RGDS (cell-adhesive peptide). PEG Control = PEG-DA hydrogel (3.4k g/mol) prepared from an aqueous precursor solution. [Scale bars = 50 μm].

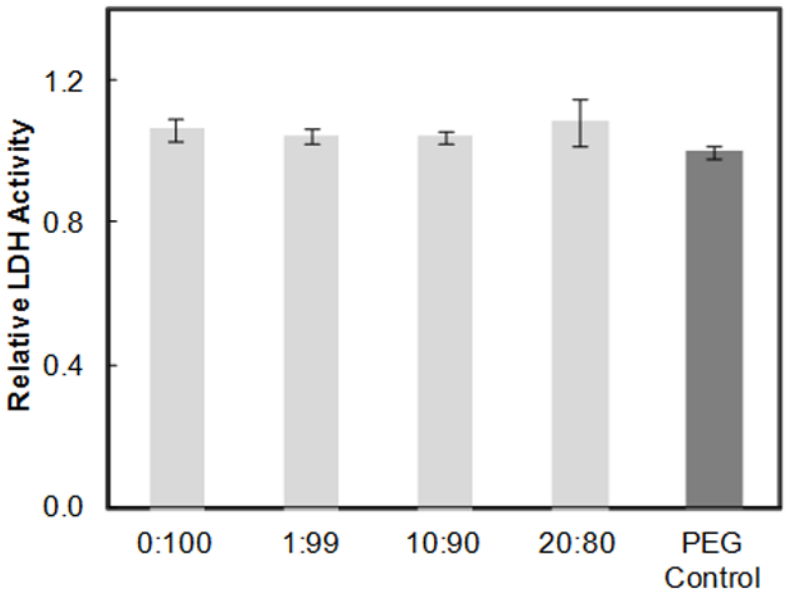

Figure 9.

Relative LDH activity (24 hr) of $PDMS_{star}$-PEG hydrogels fabricated with 3.4k g/mol PEG-DA from a DCM precursor solution (i.e. *via* SIPS) with varying wt% ratio $PDMS_{star}$-MA:PEG-DA. PEG Control = PEG-DA hydrogel (3.4k g/mol) prepared from an aqueous precursor solution. All formulations were statistically similar versus each other (ANOVA, $p < 0.05$).

Table 1.

Hydrogel Swelling Ratio and Adsorption of BSA Protein

Hydrogel formed by SIPS	Swelling Ratio	mg BSA adsorbed per cm^2 (x 10^{-4})[b]	Hydrogel formed in water[a]	Swelling Ratio	mg BSA adsorbed per cm^2 (x 10^{-4})[b]
M_n = 3.4k g/mol (PEG-DA)			*M_n = 3.4k g/mol (PEG-DA)*		
$PDMS_{star}$-PEG wt%			**$PDMS_{star}$-PEG wt%**		
0:100	7.2 ± 0.01	2 ± 0.4	**0:100**	8.6 ± 0.02	5 ± 1
1:99	7.0 ± 0.04	25 ± 2	**1:99**	8.5 ± 0.03	14 ± 6
10:90	5.7 ± 0.04	10 ± 3	**10:90**	7.8 ± 0.02	6 ± 3
20:80	4.9 ± 0.09	19 ± 6	**20:80**	7.6 ± 0.09	19 ± 2
PEG M_n = 6k g/mol (PEG-DA)			*PEG M_n = 6k g/mol (PEG-DA)*		
$PDMS_{star}$-PEG wt%			**$PDMS_{star}$-PEG wt%**		
0:100	9.8 ± 0.09	10 ± 7	**0:100**	9.3 ± 0.2	12 ± 5
1:99	9.1 ± 0.10	16 ± 2	**1:99**	9.7 ± 0.1	15 ± 2
10:90	7.6 ± 0.06	11 ± 2	**10:90**	9.2 ± 0.1	13 ± 3
20:80	6.5 ± 0.13	19 ± 6	**20:80**	8.8 ± 0.1	10 ± 1

[a] Prepared from an aqueous precursor solution

[b] Data taken from ref 60.